Different Types of Signal Coupling in the Visual Cortex

Related to Neural Mechanisms of Associative Processing and Perception

R. Eckhorn, A. Gail, A. Bruns, A. Gabriel, B. Al-Shaikhli, and M. Saam

Philipps-University, Physics Department, Neurophysics Group, D-35032 Marburg, Germany

Corresponding author: Reinhard Eckhorn
Philipps University Marburg, Physics Dept., Neurophysics Group
Renthof 7, 35032 Marburg, GERMANY
phone: ++49 6421 28-24164
fax: ++49 6421 28-27034
email: Reinhard.Eckhorn@Physik.Uni-Marburg.de

Abstract. The hypothesis of object representation by synchronization in visual cortex has been supported by our recent experiments in monkeys. They demonstrated local synchrony among rhythmic or stochastic γ-activities (30–90 Hz) and perceptual modulation, according to the rules of figure-ground segregation. However, γ-synchrony in primary visual cortex is restricted to few millimeters, challenging the synchronization hypothesis for larger cortical object representations. The spatial restriction is due to γ-waves, traveling in random directions across the object representations. Phase continuity of these waves may support the coding of object continuity. Interactions across still larger distances among cortical areas in human data involved amplitude envelopes of γ-signals. Based on models with spiking neurons we discuss potentially underlying mechanisms: (i) Fast inhibitory feedback loops generate locally synchronized γ-activities. (ii) Hebbian learning of connections with distance-dependent delays explains the stabilization of cortical retinotopy, the limited size of synchronization, the occurrence of γ-waves, and the larger receptive fields at successive levels. (iii) Slow inhibitory feedback supports figure-ground segregation. (iv) Temporal dispersion in far projections destroys coherence of fast signals but preserves slow amplitude modulations. In conclusion, we propose that the hypothesis of object representation by γ-synchronization be extended to more general forms of signal coupling and associative processing.

KEYWORDS: feature binding, scene segmentation, synchrony, gamma activity, amplitude envelope

I. Temporal Coding by Different Types of Signal Coupling in the Visual Cortex

There are two basic possibilities for testing the presence and relevance of neural temporal coding on the basis of signal recordings from perceptual systems. One can measure how well the putative temporal code correlates (i) with the properties of a sensory stimulus or (ii) with the perceptual or behavioral response to the stimulus. It is an open question which statistical measure is adequate for a certain situation (e.g., mutual information [1]), which signal types provide the best insight (e.g., intracellular membrane potentials, single unit spike trains, or population signals including multiple unit activity or local field potentials; cf. Appendix), or which signal parameters are relevant (e.g., average rate vs. precise spike timing, signal power or coupling in certain frequency bands, etc.). However, if we can develop neural models that are biologically plausible and appropriate for the investigated sensory or cognitive task, we can carry out such measurements also in these models, and systematically identify the signals and model components influencing the validity of a special temporal code. This approach is partially followed in this work about aspects of temporal coding in the visual cortex.

In our view of the visual system, temporal coding is intimately linked to the neural mechanisms of dynamic cortical cooperativity, including the largely unknown mechanisms of perceptual feature binding and, in general, the interaction among different levels of visual processing. How are local features flexibly grouped into actually perceived objects and events, and how do their current representations interact with visual memory and other higher-order processes? It has been proposed that binding of spatially distributed features and inter-areal cooperation are supported by the temporal code of fast synchronization among neurons involved in a common task, for example, the coding of a visual object [2, 3]. This hypothesis attracted attention when synchronized γ-oscillations (30–90 Hz) were found in the primary visual cortex (V1) of anesthetized cats [4, 5, 6] and awake monkeys [7, 8]. Many subsequent experiments were supportive, some challenging with respect to binding of local features by γ-synchronization (reviews, e.g., [9, 10]). For example, synchronization of signals in the γ-range was found to be restricted to few millimeters in primary visual cortex, even with large coherent stimuli [6, 11]. According to a strict interpretation of the

original synchronization hypothesis, this should result in locally restricted perceptual feature binding. But this is in contradiction to the capability of perceiving the local features of large objects as coherently bound. However, the capability of far-range feature binding across the surface of a large visual object is probably due to a continuous binding among overlapping regions of locally restricted feature binding (as demonstrated by the perceptual laws of Gestalt psychology; e.g., [12]). Accordingly, we suggest phase *continuity* of signals in the γ-range (as opposed to strict synchrony), as a less restrictive type of signal coupling within retinotopically arranged cortical areas, to be a basis of spatial feature binding across entire objects. Such phase coupling has been found to cover larger cortical ranges than γ-synchrony [13, 14], and we will argue why it probably fills the entire surface representation of visual objects in primary visual cortex.

While the spatial range of lateral signal coupling in topographically organized maps can be extended by the above mentioned phase continuity coding, such continuity may not be available between separate topographical maps (here: different visual cortical areas). However, γ-synchronization has been found between neural groups with overlapping receptive fields in adjacent visual cortical areas V1 and V2 in cats [4, 6] and monkeys [8]. It is probable that such synchrony is also present among other visual areas when the feed-forward-backward delays are short (i.e., when the areas are close to each other in temporal coding space, e.g., as between V1 and MT [15]). In contrast, cooperativity between cortical areas that are far apart in temporal coding space (due to long reciprocal conduction delays) may be reflected in other forms of signal coupling which are less sensitive to any spatio-temporal restriction of synchronization. This assumption is motivated by the fact that different spike conduction velocities within an axonal bundle are likely to cause temporal dispersion of population activity during transmission [15] and thus destroy the synchrony of the associated signals. Therefore, completely disregarding the phase structure and solely concentrating on the time-varying amplitude (*amplitude envelope*) of γ-signals seems to be a particularly promising approach, which will be detailed in the present article.

For our present work different types of neural signals have been recorded, and different forms of temporal coding have been investigated by means of various frequency selective coupling measures (cf. Appendix). We will demonstrate dynamic coupling of cortical signals in the form of

local intra-areal phase synchrony, medium-range phase continuity of γ-waves, and long-range coupling involving amplitude envelopes of γ-signal components. We will give examples for the correlation of physiological measures with sensory events, with perceptual and behavioral outputs, and with cognitive states, in monkeys and humans. In essence, we argue that the temporal coding hypothesis of binding-by-synchronization, initially restricted to γ-synchrony of oscillatory signals, has to be extended to more general forms of temporal coding, including non-linear signal coupling across the entire frequency range of cortical activity with phase- and amplitude-coupling among transient and stochastic (non-rhythmic) signals. On the basis of neural models with spiking neurons we will discuss most of the physiological results and suggest potential neural mechanisms underlying the presented types of temporal coding.

II. Experimental Evidence

A. γ-Activity in Monkey Primary Visual Cortex is Phase-Coupled within Representations of Scene Segments and Decoupled Across their Contours.

The binding-by-synchronization hypothesis suggests coupling among γ-activities representing the same object, or more generally, the same scene segment. Accordingly, neural groups representing different scene segments should decouple their γ-activities. Both predictions have been tested by investigating the effect of a static figure-ground stimulus on local field potentials (LFPs; see Appendix) in primary visual cortex (V1) of awake monkeys, recorded simultaneously from inside and outside a figure's representational area [16] (Fig. 1A). Time-resolved analysis of phase coupling by means of spectral coherence revealed: (i) γ-coherence between neurons representing the same scene segment (figure or ground) is higher than for a homogeneous gray background of the same average luminance (Fig. 1B,D); (ii) stimulus-specific γ-coherence is strongly reduced across the representation of the figure-ground contour compared to a spatially continuous stimulus (Fig. 1B,D); (iii) decoupling across the contour emerges with a latency of about 100 ms, and is absent in the earliest neuronal response transients (Fig. 1D); (iv) coherence of low-frequency components does not

show a difference between the figure-ground and the continuous condition (not shown). We propose that the increased γ-coherence between neurons representing the same scene segment and the decoupling of γ-activity at a contour representation are crucial for figure-ground segregation, in agreement with the initial binding-by-synchronization hypothesis.

B. γ-Phase Coupling in Monkey Extra-striate Cortex Correlates with Perceptual Grouping.

Are such synchronization effects correlated with perceptual feature grouping and figure-ground segregation? This was tested in a difficult figure-ground task in which a monkey indicated whether he perceived a figure composed of blobs among identical distractor blobs serving as background [17] (Fig. 2). This task was sufficiently difficult such that about 25 % of responses were incorrect (failed figure detection). Pairs of local populations of figure-activated neurons in visual area V2 showed increased synchronization within the γ-range in correct compared to incorrect responses during a short period before the monkey's behavioral response (Fig. 2). Other signal measures were unrelated to perception. These were the first indications that γ-synchronization in V2 may not only represent physical stimulus properties but also support perceptual grouping.

C. Phase Coupling in Low and Medium Frequency Ranges in Monkey Primary Visual Cortex Correlates with States of a Bistable Percept.

Another study investigated relations among synchronization in primary visual cortex (V1) and perceptual grouping, using conditions of bistable perception [18]. Monkeys reported their alternative percepts among dichoptically presented, incongruent (and hence rivalrous) grating stimuli of orthogonal orientations. During congruent (non-rivalrous) stimulation, γ-power and γ-coherence of LFP-signals in V1 were modulated depending on the grating orientation, as in previous work (e.g., [11, 19]). During incongruent (rivalrous) stimulation LFPs were often correspondingly modulated in consonance with the changing perceptual state, although the visual stimulus was constant (Fig. 3). These perception-related modulations occurred at low and medium (4-27 Hz), but barely at γ-frequencies (28-90 Hz).These results are at odds with the concept of feature-linking by γ-synchrony,

but not with a more general role of synchrony for perceptual binding that includes low and medium frequencies. The somato-dendritic nature of the perception-related signal components (modulation of LFPs, but not population spike density), together with their latency led us to the assumption that these modulations are driven by top-down signals to area V1 from other cortical areas already representing or carrying a prediction about the oncoming perceptual state. Such long-range inter-areal interactions may be carried by slower signal components (< 30 Hz; cf. Section III) than local processing based on fast γ-range signals.

D. Phase Continuity but not Synchrony of γ-Waves is Present Across Medium Cortical Distances in Monkey Primary Visual Cortex.

Previous work demonstrated that the synchronization range of γ-activity in primary visual cortex is limited to about 5 mm (e.g., [11, 20, 21] and Fig. 6A). Hence, objects with larger cortical representations can not solely be coded by γ-synchrony within their representational area. One explanation for the limited synchronization range lies in the spatio-temporal characteristics of γ-activity. In fact, wave-like phenomena defined by spatially continuous phase-fronts (*γ-waves*) do extend farther than 5 mm, but phase differences between any two sites change randomly already within 100 ms and also increase with cortical distance (Fig. 4A) [13, 14]. Conventional pairwise coupling measures (cross-correlation, coherence; cf. Appendix) do not capture such non-trivial phase relationships across medium-range cortical distances, which explains the findings of restricted synchronization ranges. To quantify those waves a new method has been developed in our group ([13, 14]; Appendix). It revealed that γ-waves travel at variable velocities and directions. Figure 5 shows the velocity distribution measured with a 4×4 microelectrode array in monkey V1 during retinally static visual stimulation. Note that this distribution is rather similar to the distribution of spike velocities of horizontal connections in V1 [15]. We suggest that continuity of γ-waves supports the coding of object continuity, in which case their extent over object representations in visual area V1 and the related visual fields should be much larger than that covered by γ-synchronization. This has indeed been found (Fig. 6A,B).

E. Far-Range Coupling Involving Amplitude Envelopes of γ-Signals in Human Cortex Depends on Cognitive States.

High-frequency processes seem to be mainly relevant for local aspects of stimulus processing, as in many cases they show a spatially limited synchronization range. This was not only observed in microelectrode recordings from monkey cortex [11, 20, 21], but also in intracranial recordings from human cortex [22, 23, 24, 25]. In the following we will present a perspective that goes beyond lateral cooperativity within one cortical area or cooperativity between homologous sites of different representational maps. Results from human subdural recordings suggest a special role of amplitude envelopes of γ-range signals in long-distance signal coupling. Investigating the correlation between amplitude envelopes of γ-bandpass-signals (γ-*envelopes*) has been shown to be a useful method for capturing coupling events even during the absence of γ-coherence (*envelope correlation*, [26]). Similarly, correlation between low-frequency signals and γ-envelopes has turned out to be another efficient measure of cortico-cortical signal coupling (*envelope-to-signal correlation*, [27]). For comparing the spatial range of different coupling measures in intracranial signals, subdural recordings from human subjects are especially suitable, since they cover comparatively large cortical regions. Fig. 7 shows the incidence of event-related coupling changes of coherence and envelope-based coupling measures during performance of a visual delayed-match-to-sample task. The results demonstrate that (i) a notable dissociation between coupling measures occurs only in the γ-frequency range, where amplitude-based signal coupling is generally more responsive to sensory and cognitive events than phase coupling (upper row); (ii) in the γ-range, the incidence of coupling events involving envelopes drops off less rapidly with distance than that of phase coupling events (upper row, right diagram); (iii) the incidence of envelope-to-signal correlation events depends on the cognitive task even for large inter-electrode distances, whereas task-dependence in the other coupling measures occcurs only within a spatial range of a few centimeters (lower row).

III. Potential Neural Mechanisms of Flexible Signal Coupling

At present it is not possible to identify directly from experimental measurements the neural mechanisms underlying the above mentioned experimental observations of spatio-temporal processing in cortical sensory structures. We therefore use largely reduced model networks with spike-coding neurons to discuss potential mechanisms.

A. Synchronization of Spike Densities in Local Populations by Feedback Inhibition

The first question we ask is: how may fast signals in the γ-range, including their rhythmic states, be generated? We argue in Fig. 8 that membrane potentials of local populations of excitatory neurons are simultaneously modulated by inhibition exerted via a common feedback loop (physiology: [28, 29, 30]; models: [31, 32, 33, 34]; discussion in [35]). This loop can quickly reduce transient activations, whereas sustained input will lead to repetitive inhibition of the population in the γ-frequency range (Fig. 8). In both modes – transient and rhythmic chopping – the common modulation of the neurons' membrane potentials causes their spike trains to become partially synchronized, even if they fire at very different rates. The stronger a neuron is activated and depolarized, the earlier it will discharge its first spike during the common repolarization phase, whereby such a population burst will be dominated by the most strongly activated neurons. As local cortical populations generally project to common targets [36], synchronized spike densities (*population spike packages*) will have stronger impact there than uncorrelated spike densities of equal average amplitudes, because they (i) appear quasi-simultaneously, and (ii) mainly comprise spikes of strongly activated neurons, which represent the stimulus at a better signal-to-noise ratio than the neurons that were activated weaker by the same stimulus.

We can apply this scheme to the primary visual cortex, where local neural clusters represent similar feature values (e.g., receptive field position, contour orientation, etc.). According to the synchronization hypothesis, partial synchronization of spike densities by a common inhibitory feedback means that currently present local combinations of visual feature values are systematically

selected by their strength of activation and tagged as belonging together, which is comprised in single or repetitive population discharges.

B. Lateral Conduction Delays can Limit γ-Synchrony to Few Millimeters in Cortex, Produce Wave-Like Phenomena, Stabilize Cortical Topography, and Lead to Larger Receptive Fields at Successive Levels of Processing

In primary visual cortex there are dense horizontal connections monosynaptically projecting over a range of several hypercolumns [37, 38]. One could suppose that simultaneously activated neural populations representing the entire surface of a visual object might all synchronize their spike packages via these horizontal connections. As mentioned in Section II-D, however, γ-synchrony is restricted to about 5 mm cortical distance (corresponding to 5 hypercolumns), even if the cortical representation of a visual object is much larger [6, 11]. Hence, γ-synchrony for feature binding would be restricted to visual objects being not larger in their cortical representation. In the following we will develop a concept of how distance-dependent spike conduction delays can explain this restricted range of γ-synchrony and the occurrence of wave-like phenomena in a network of spiking neurons. Hebbian learning combined with distance-dependent spike conduction delays leads to spatially restricted lateral connectivity within a layer and restricted feed-forward divergence between layers. Therefore, such a mechanism is also suitable to explain the emergence of larger receptive fields at successive levels of processing while preserving a topographical mapping.

1) Hebbian-Learning Model with Finite Conduction Velocities. The model [39] consists of spike-coding neurons at two successive, 2-dimensional retinotopic visual processing stages named level-1 (representing visual cortical area V1) and level-2 (V2) (Fig. 9). Learning of lateral coupling weights and level-1-to-level-2 weights is implemented using a Hebbian correlation rule [40]. Feed-forward connections are additive and determine the properties of the classical receptive fields. Lateral connections are multiplicatory, i.e., modulatory, which means they cannot directly evoke spikes in a target neuron, but require quasi-simultaneous feed-forward input to that neuron (model: [41]; physiology: [42]). Spikes evoked by quasi-simultaneous feeding input to neighboring neurons

can synchronize via their modulatory mutual lateral connections because these spikes will often occur within the so-called *capture range* of the spike encoder's dynamic threshold [41,43,44]. However, lateral connections in the model have finite conduction velocities such that, with increasing distance, conduction delays become larger. This reduces the probability of neurons becoming quasi-synchronized because constructive superposition of locally evoked and laterally conducted activities gets less probable for increasing delay. Hence, synchrony is laterally restricted to a spatial range which is proportional to the conduction velocity of the lateral connections.

2) Spatio-Temporal Structuring of Lateral Connectivity with Hebbian Learning. The relation between conduction velocity and synchronization range suggests an influence of *temporal neighborhood* (defined by the distance-dependent delays) on the ontogenetic, possibly prenatal formation of functionally relevant structures from an initially unstructured system. This effect can be simulated with the model. In the beginning, neurons are fully interconnected within level-1 (Fig. 9, scenario A). Feed-forward input spike trains have spatially homogenous random patterns and are given a temporally confined, weak co-modulation, mimicking activity before visual experience. This type of spike pattern appears, slightly modified by the connections, at the output of the level-1 neurons (Fig. 10) and hence, is used for Hebbian learning. The only topography in the network is given by the distance-dependent time delays of the lateral connections. During a *first learning period*, the homogeneous coupling within layer-1 shrinks to a spatially limited coupling profile for each neuron, with a steep decline of coupling strength with increasing distance (Fig. 11). The diameter of the resulting coupling profile for each neuron is equal to the lateral synchronization range, and hence directly proportional to the lateral conduction velocity (Fig. 12).

3) Spatio-Temporal Structuring of Inter-Level Connectivity. In a *second learning period* following the learning period within level-1, the feed-forward level-1-to-level-2 connections are adapted, also starting from full connectivity (Fig. 9, scenario B). As a result of Hebbian correlation learning, the feed-forward divergence retracts to a limited spatial range which is given by the size of level-1 synchronization fields, i.e., forward connections from neurons within a level-1 synchronization field (sending near-synchronized spike packages) converge onto one level-2 neuron (Fig. 13). This convergent projection pattern even emerges if the feed-forward connections and the

level-2 lateral connections are modeled with distance-independent constant delays (Fig. 9, scenario C). The physiological interpretation of this result is that the size of level-1 (visual area V1) synchronization fields can determine the size of level-2 (area V2) receptive fields. Indeed, synchronization fields in area V1 and classical receptive fields in area V2 of the monkey do have similar sizes. Since equivalent considerations should hold for projections from the retina to V1, the model accounts for the emergence not only of a spatially regular, but also of a retinotopically organized connectivity.

4) Traveling γ-Waves with Altering Phase Relations. After having learned the lateral synaptic weight profiles, the model reproduces the phenomenon of waves with jittering phase relations, traveling in random directions, just as it was observed in the primary visual cortex (Fig. 4) [14, 45]. Traveling waves of γ-activity, though concentrically expanding, have already been described in different cortical areas of different animal species (e.g., [46]). The varying phase relations in the model as well as the more rapid spatial decline of γ-coherence (compared to γ-wave probability) are consistent with the experimental data (Figs. 4, 6). Formation of γ-waves in the model results from locally restricted inhibition, lateral conduction delays, and steep spatial decline of coupling strength [39]. It seems probable that γ-waves in *physiological* signals are also strongly depending on the slow lateral conduction velocities, because the distribution of γ-wave velocities (Fig. 5) is similar to the distribution of spike conduction velocities of lateral connections in primary visual cortex. These velocities have been estimated in different preparations, including rat slices and *in vivo* recordings from cats and monkeys, to range between 0.1 and 1.0 m/s (review: [15]).

In conclusion, low lateral cortical conduction velocities, combined with Hebbian correlation learning, can explain the restricted spatial range of γ-synchrony and the occurrence of traveling γ-waves with random phase relations. They can also account for the larger receptive fields at higher processing levels and for the emergence and stability of topographic visual (and other sensory) representations without the need for visual (sensory) experience. During visual experience, of course, similar influences on synchronization-field and receptive-field size and on topographic stability may be operative at successive levels of processing, including other parts of the visual system. As the traveling waves probably can cover the entire representation of an object's surface in the primary

visual area, we propose that *phase continuity* of γ-waves may constitute a mechanism that supports the coding of *object continuity* in visual cortex [13].

C. Model Explaining Figure-Ground Segregation and Induced Modulations at Lower Frequencies by Slower and More Globally Acting Feedback Circuit

In a further approach the above model of the visual cortex has been expanded by using orientation-selective excitatory neurons and two types of inhibitory neurons with different spatio-temporal properties. However, the lateral connections among the excitatory neurons were modeled without delay and learning has been excluded in order to keep the complexity of the network within limits in order to understand its processing. Figure 14 shows a simplified wiring diagram of this model. The spiking neurons have linearly and nonlinearly acting synapses and are retinotopically arranged in two primary layers with receptive fields at perpendicular orientation preferences. Additionally to a fast within-layer inhibitory feedback loop, responsible for the local chopping of activity at γ-frequencies (see above and Fig. 8), orientation-independent slow shunting inhibition is common to both orientation layers in this model.

1) γ-Decoupling Across Figure-Ground Contour. In the figure-ground experiment, representations of different scene segments in primary visual cortex (area V1) were decoupled in their γ-activities (Fig. 1B,D), while the same sites showed substantial γ-coupling when representing one coherent scene segment. Analogous results are obtained with the model (Fig. 1C,E). It explains the reduced γ-coherence as a blockade of lateral coupling at the position of the contour representation due to several effects: First, neurons responding preferentially to the horizontal grating are only weakly activated by the vertical contour. Second, their activity is even more reduced by the orientation-independent slow shunting inhibition, induced by the strongly activated vertically tuned neurons at the contour. As a consequence, neurons activated by the horizontal grating near both sides of the contour can not mutually interact, because orientation-selective lateral coupling is interrupted by the inhibited horizontally tuned neurons at the contour representation. The resulting decoupling of inside and outside representations is not present during the first neural response

transient after stimulus onset (Fig. 1D,E), since the sharp, simultaneous response onset common to both orientation layers denotes a highly coherent broad-band signal which dominates internal dynamics. Note that orientation-selectivity was implemented for the sake of comparability with the experimental data. This does not limit the general validity of this model, since any object border constitutes a discontinuity in at least one visual feature dimension, and therefore an analogous argumentation always holds for other local visual features.

2) Perception-Related Low-Frequency Modulations with Bistable Stimuli. In experiments with binocular rivalry always one of two dichoptically presented overlapping visual objects dominates perception. Perception-related modulations of signals and of their phase coupling occurred mainly in the low-frequency range, to a lesser degree at medium frequencies, and barely at γ-frequencies in the primary visual cortex of monkeys [18]. At the same time, stimulus-related modulations of γ-activity were strongly present. This stimulus-specificity of high- and low-frequency components, and the perception-specificity of only low-frequency signal components may also partly be explained on the basis of our model in Figure 14: The relatively slow shunting-inhibition loop, shared by both layers of orientation-selective neurons, can produce single or, with sustained sensory drive, repetitive low-frequency modulations of population activities. However, the selective perception-related increase of these slow components (Fig. 3) requires an external perception-related signal that selectively amplifies, for example, the excitability of neurons representing the currently dominating grating. This signal could be fed with positive sign to the modulatory linking inputs acting on the feed-forward inputs (Fig. 14A) via a multiplicative stage ("Π" in Fig. 14B). Indeed, the physiological results partly were indicative for a top-down influence on area V1 to explain the perception-related modulations (cf. Section II-C). Such imbalanced, sustained input to lateral linking connections would also enhance the lateral coupling strength in the respective orientation layer, which may support perceptual dominance of the grating with the corresponding orientation.

D. Spatial and Temporal Aspects of Object Representations

We have seen that within an object's representation in primary visual cortex, locally synchronized γ-activations emerge that overlap in space and time and thereby support the formation of γ-waves traveling across the object's surface representation with random phase relations. When waves of γ-activity travel across V1, this is paralleled by quasi-synchronous activity of those V2-neurons having corresponding receptive field positions [4, 6, 8], i.e., those receiving input from, and sending γ-feedback to, corresponding V1-neurons. Thus, adjacent V2-neurons, driven simultaneously by adjacent parts of a traveling wave, will also form a traveling wave of γ-activity (with similar extent, velocity and direction if projected to visual space). We expect such an argumention to hold for subsequent stages of processing, provided that they are retinotopically arranged, are activated by bottom-up input, and have fast inter-areal feedback (compared to a half-cycle of a γ-wave). Accordingly, quasi-synchrony should generally be present among neurons with overlapping receptive field positions across cortical levels connected via fast feed-forward-backward loops (e.g., as among V1-V2 and V1-MT [15, 47]). Based on the observed γ-decoupling across a figure-ground contour (Section II-A), we suppose that these waves are damped off at object contour representations, i.e., they can not pass them. Continuity across the entire representation of an object then could be coded by traveling waves of γ-activity that appear simultaneously in several areas. *Object continuity* may thus be coded by *phase continuity* of traveling γ-waves.

E. Far-Range Cooperation is Mediated by Amplitude Envelopes of γ-Range Signals

Especially when inter-areal cooperativity across large cortical distances is concerned, it is probable that different conduction velocities and/or activation delays within a population of projecting neurons lead to temporal dispersion of spike patterns as they were at the source site [15]. Such a dispersion would reduce signal coherence between source and target site primarily in the γ-frequency range, because the superposition (i.e. average) of high-frequency signals is more sensitive to a given temporal jitter than that of low-frequency signals. It is therefore interesting that, based on electrophysiological findings, some authors have proposed that coupling between high-frequency

signals might reflect local cooperative processing, whereas coupling between low-frequency signals could be associated with global, i.e., long-range interactions in higher cognitive functions (e.g. [48, 49]; cf. also section II-C). In a further step of argumentation, nonlinear interactions between fast and slow signal components have been suggested to reflect the functional integration of local and global neural processes [22, 48, 50, 51].

Based on these arguments, we propose that signal coupling involving slow amplitude modulations of fast signals (γ-activity) may serve as a valuable indicator of neural long-distance interactions for two reasons. First, amplitude modulations represent a special and very intuitive form of inter-frequency interaction. Second, signal coupling involving such modulations is less sensitive to temporal dispersion than coupling involving high-frequency signals proper. This may primarily apply to cases in which effective transmission delays are long and Hebbian learning (see above) has not led to a selection of fibres with equal conduction velocities.

A simple mechanistic concept (Fig. 15) is able to account for the occurrence of γ-envelope-to-signal correlation between subdurally recorded local field potentials, which was particularly cognition-dependent (cf. Fig. 7). These signals mainly reflect a spatial (*ensemble*) average of dendritic membrane potentials (Appendix), whose high-frequency fluctuations in turn have considerable influence on the spike patterns: While their *amplitude* correlates with the spiking *probability* [52, 53], their *phase* structure determines the precise *timing* of the spikes [53]. We can therefore suppose that the amplitude envelope of the measured γ-signal (upper left part of Fig. 15) reflects the temporally smoothed overall spike density within the source population, whereas the fine temporal structure of the γ-signal determines the precise temporal spike pattern within the ensemble (lower left part of Fig. 15). During spike propagation to a remote common target, even slightly different conduction velocities within the axon population will cause temporal dispersion of the spikes and thus destroy the temporal structure of the ensemble spike density (lower right part of Fig. 15). The dispersed activities will elicit post-synaptic potentials in the target population, which in turn will superimpose to make up (part of) the subdural signal recorded there (upper right part of Fig. 15). As a consequence of temporal dispersion, γ-coherence between the two recording sites will be low. On the other hand, slow modulations of the temporally smoothed spike density, as reflected

by γ-envelopes at the source site, will correspondingly modulate the amount of post-synaptic potentials elicited at the target site, which in turn will be directly reflected in the sum potential recorded there. This effect causes correlated time courses of source-site γ-envelopes and target-site low-frequency signals.

IV. Appendix – Definition of Synchrony and Correlation Measures, and Characterization of Recorded Signals

A. Synchrony

In the present context the terms *synchrony* and *synchronization* are related to temporal properties of neurons, in particular to postsynaptic *integration time*. In a first approximation the integration time can be estimated as the half-height duration of an average excitatory postsynaptic potential. When multiple presynaptic action potentials arrive within the integration time of a neuron, we will call them *synchronized*. Integration times can differ in different neurons, in a single neuron at different synapses, and they can change dynamically. The latter effects depend on postsynaptic membrane properties and on the temporal patterns of spike input [42, 54, 55, 56]. In cortical neurons integration times can span the broad range of 2–100 ms. In the activated cortex of awake mammals, in which we are interested in the present paper, integration times are estimated as ranging within 5–50 ms (for a review see [57]).

Synchronized neural events may occur singly, or repetitively with a more stochastic or rhythmic (oscillatory) character. At a target neuron, synchronized excitatory input spike patterns produce higher and steeper membrane depolarization than temporally dispersed inputs of the same average spike density. Hence, synchronization increases the output spiking probability [57, 58, 59, 60] and also facilitates preservation of transmitted temporal spike patterns. Depending on the temporal synchronization range imposed by the aforementioned integration times, synchrony can show up in different frequency bands of physiological signals. Synchronization on a temporal scale of 5–15 ms,

for example, corresponds to the so-called *gamma* (γ-) range (30–90 Hz), and will therefore be termed γ-synchronization.

B. Recorded Neural Signals

The neural signals in the present work were either recorded extracellularly with multiple microelectrodes from awake monkeys or subdurally from human subjects (cf. below). Monkey data are based on local population activity contained in multiple unit activity (MUA), and local field potentials (LFP). MUA and LFP were generally recorded by the same microelectrode. Broad-band signals were band-passed (1–10 kHz) to extract the spike activities. Further processing consisted of full-wave rectification and low-pass filtering at 140 Hz to obtain a continuous signal that is proportional in its amplitude to the extracellularly averaged spike densities of neurons near the electrode tip (half decline radius about 50 µm) [61, 62]. For LFP only band-pass filtering (0.1–140 Hz) of broad-band signals was used to obtain extracellularly averaged postsynaptic potentials (half-decline radius about 400 µm) [63]. Due to the extracellular superposition, MUA and LFP amplitude increases as synchronization of the contributing neural signals becomes more precise. This means MUA and especially LFP recordings are *per se* sensitive probes for synchronized activity in the neural population contributing to the signals. But they are also more sensitive to coupling among separated neural populations than are single unit spike trains. Even during fast oscillations, i.e., states of high γ-synchrony within a neural population, single unit spike activity is only weakly coupled to the group signals [64].

In principle, the same considerations hold for subdurally recorded signals from human cortex. They also mainly reflect a spatial (ensemble) average (i.e., the correlated proportion) of dendritic activity near the electrode [65]. However, they represent neural activity from within a radius of approximately 5 mm and thus comprise postsynaptic activities of millions of neurons each. Given this comparatively poor spatial resolution, assigning subdural recording sites to certain positions in the visual field is hardly possible.

C. Different Forms of Signal Coupling Quantified by Appropriate Measures

Cortical interaction has to serve various functions, and has to meet different spatial and temporal requirements. Therefore, cortical interaction will certainly be based on a variety of neural mechanisms. It would be naive to expect a single type of temporal coding, e.g. phase synchronization in the γ-range, to be indicative for any form of cooperativity. For the present paper, we therefore used different coupling measures which are all selective for signal frequencies. The main difference between the measures concerns their sensitivity for the signals' phase structure. To quantify *synchrony* we used spectral *coherence* [66]. High coherence requires a phase difference between two signals which has to be constant (but not necessarily zero) over time. Thus, synchrony in this context does not mean precise coincidence of events, but it still indicates a temporally stable phase relationship. Coherence determines linear coupling at each frequency independently. To quantify *phase continuity*, i.e., to detect *traveling waves*, we used a new and highly adapted multi-channel correlation method [13, 14]. This method, in contrast to coherence or cross-correlation, allows variable relative phases over time between two separated recording positions. But within each short time interval (20 to 40 ms) the phase gradient across space has to be constant. For example, signals obtained from linearly arranged, equidistant recording positions need to have phase differences proportional to the distance of the recording positions. In a third approach we quantified non-linear coupling through correlations between amplitude *envelopes* of band-pass signals in various frequency bands [26] or between such envelopes and *slow signals* [27]. This measure is completely independent of the signals' phases. Note that for model data we mimic the physiological signal types and use exactly the same measures for analysis of both types of data.

References

[1] C. E. Shannon, “A mathematical theory of communication,” *Bell Syst. Tech. J.*, vol. 27, pp 623–656, 1948.

[2] H. J. Reitboeck, “A multi-electrode matrix for studies of temporal signal correlations within neural assemblies,” In *Synergetics of the Brain*, E. Basar et al., Eds. Berlin: Springer, 1983, pp. 174–182.

[3] C. von der Malsburg and W. Schneider, “A neural cocktail-party processor,” *Biol. Cybern.*, vol. 54, pp. 29–40, 1986.

[4] R. Eckhorn, R. Bauer, W. Jordan, M. Brosch, W. Kruse, M. Munk, and H. J. Reitboeck, “Coherent oscillations: a mechanism of feature linking in the visual cortex? Multiple electrode and correlation analyses in the cat,” *Biol. Cybern.*, vol. 60, pp. 121–130, 1988.

[5] C. M. Gray, P. König, A. K. Engel, and W. Singer, “Oscillatory responses in cat visual cortex exhibit inter-columnar synchronization which reflects global stimulus properties,” *Nature*, vol. 338, pp. 334–337, 1989.

[6] R. Eckhorn, “Oscillatory and non-oscillatory synchronizations in the visual cortex of cat and monkey,” in *Oscillatory Event-Related Brain Dynamics*, C. Pantev, T. Elbert, and B. Lütkenhöner, Eds. New York: Plenum Press, 1994, pp. 115–134.

[7] A. Kreiter and W. Singer, “Oscillatory neuronal responses in the visual cortex of the awake macaque monkey,” *Eur. J. Neurosci.*, vol. 4, pp. 369–375, 1992.

[8] A. Frien, R. Eckhorn, R. Bauer, T. Woelbern, and H. Kehr, “Stimulus-specific fast oscillations at zero phase between visual areas V1 and V2 of awake monkey,” *Neuroreport*, vol. 5, pp. 2273–2277, 1994.

[9] C. M. Gray, “The temporal correlation hypothesis of visual feature integration: still alive and well,” *Neuron*, vol. 24, pp. 31–47, 1999.

[10] R. Eckhorn, “Neural mechanisms of visual feature binding investigated with microelectrodes and models,” *Vis. Cogn.*, vol. 6, pp. 231–265, 1999.

[11] A. Frien and R. Eckhorn, “Functional coupling shows stronger stimulus dependency for fast oscillations than for low-frequency components in striate cortex of awake monkey,” *Eur. J. Neurosci*, vol. 12, pp. 1466–1478, 2000.

[12] M. Wertheimer, *Untersuchungen zur Lehre von der Gestalt: II. Psychologische Forschung*, vol. 4, 1923, pp. 301-350.

[13] R. Eckhorn and A. Gabriel, “Phase continuity of fast oscillations may support the representation of object continuity in striate cortex of awake monkey,” *Soc. Neurosci. Abs.*, vol. 25, p. 677, 1999.

[14] A. Gabriel and R. Eckhorn, “Multi-channel correlation method detects travelling gamma-waves in monkey visual cortex,” in revision.

[15] L. G. Nowak and J. Bullier, “The timing of information transfer in the visual system,” in *Extrastriate Cortex in Primates. Cerebral Cortex*, vol. 12, Rockland et al., Eds. New York: Plenum Press, 1997.

[16] A. Gail, H. J. Brinksmeyer, and R. Eckhorn, “Contour decouples gamma activity across texture representation in monkey striate cortex,” *Cereb. Cortex*, vol. 10, pp. 840–850, 2000.

[17] T. Woelbern, R. Eckhorn, A. Frien, and R. Bauer, “Perceptual grouping correlates with short synchronization in monkey prestriate cortex,” *Neuroreport,* vol. 13, pp. 1881–1886, 2002.

[18] A. Gail, H. J. Brinksmeyer, and R. Eckhorn, “Perception-related modulations of local field potential power and coherence in primary visual cortex of awake monkey during binocular rivalry,” in revision.

[19] A. Frien, R. Eckhorn, R. Bauer, T. Woelbern, and A. Gabriel, “Fast oscillations display sharper orientation tuning than slower components of the same recordings in striate cortex of the awake monkey,” *Eur. J. Neurosci.*, vol. 12, pp. 1453–1465, 2000.

[20] E. Jürgens, R. Eckhorn, A. Frien, and T. Wölbern, “Restricted coupling range of fast oscillations in striate cortex of awake monkey,” Göttingen Neurobiology Report 1996. N. Elsner, H.U. Schnitzler (eds.). Stuttgart, Georg Thieme, p. 418, 1996.

[21] M. Steriade, F. Amzica, and D. Contreras, “Synchronization of fast (30-40 Hz) spontaneous cortical rhythms during brain activation,” *J. Neurosci.*, vol. 16, pp. 392–417, 1996.

[22] T. H. Bullock, M. C. McClune, J. Z. Achimowicz, V. J. Iragui-Madoz, R. B. Duckrow, and S. S. Spencer, “EEG coherence has structure in the millimeter domain: subdural and hippocampal recordings from epileptic patients,” *Electroencephalogr. clin. Neurophysiol.*, vol. 95, pp. 161–177, 1995.

[23] V. Menon, W.J. Freeman, B. A. Cutillo, J. E. Desmond, M. F. Ward, S. L. Bressler, K. D. Laxer, N. Barbaro, and A. S.Gevins, “Spatio-temporal correlations in human gamma band electrocorticograms,” *Electroencephalogr. Clin. Neurophysiol.*, vol. 98, pp. 89–102, 1996.

[24] F. Aoki, E. E. Fetz, L. Shupe, E. Lettich, and G. A. Ojemann, “Increased gamma-range activity in human sensorimotor cortex during performance of visuomotor tasks,” *Clin. Neurophysiol.*, vol. 110, pp. 524–537.,1999.

[25] D. W. Gross, and J. Gotman, “Correlation of high-frequency oscillations with the sleep-wake cycle and cognitive activity in humans,” *Neurosci.*, vol. 94, pp. 1005–1018, 1999.

[26] A. Bruns, R. Eckhorn, H. Jokeit, and A. Ebner, “Amplitude envelope correlation detects coupling among incoherent brain signals,” *Neuroreport*, vol. 11, 1509–1514, 2000.

[27] A. Bruns and R. Eckhorn, “Task-related coupling from high- to low-frequency signals among visual cortical areas in human subdural recordings,” in revision.

[28] W. Freeman, “Distribution in time and space of prepyriform electrical activity,” *J. Neurophysiol*, vol. 22, pp. 644–665, 1959.

[29] B. A. McGuire, C. D. Gilbert, P. K. Rivlin, and T. N. Wiesel, “ Targets of horizontal connections in macaque primary visual cortex,” *J. Comp. Neurol.*, vol. 305, pp. 370–392, 1991.

[30] R. Douglas and K. A. C. Martin, “A functional microcircuit for cat visual cortex,” *J. Physiol. London*, vol. 440, pp. 735–769, 1991.

[31] C. van Vreeswijk, L. F. Abbott, and G. B. Ermentrout, “When inhibition not excitation synchronizes neural firing,” *J. Comput. Neurosci.*, vol. 1, pp. 313-321, 1994.

[32] W. J. Freeman, “Feedback models of gamma rhythms," *Trends Neurosci.*, vol. 19, pp. 468–470, 1996.

[33] P. Bush and T. Sejnowski, “Inhibition synchronizes sparsely connected cortical neurons within and between columns in realistic network models,” *J. Comput. Neurosci.*, vol. 3, pp. 91–110, 1996.

[34] T. Wennekers and G. Palm, “Cell assemblies, associative memory and temporal structure in brain signals,” in *Time and the Brain*, Series: CABR: Conceptual Advances in Brain Research, vol. 3, R. Miller, Ed. Harwood Academic Publishers, 2000, pp. 251–273

[35] R. Eckhorn, “Cortical processing by fast synchronization: high frequency rhythmic and non-rhythmic signals in the visual cortex point to general principles of spatiotemporal coding,” in *Time and the Brain*, R. Miller, Ed. Lausanne: Gordon&Breach, 2000, pp. 169–201.

[36] V. Braitenberg and A. Schuez, *Anatomy of the cortex.* Berlin: Springer, 1991.

[37] D. Y. Ts'o, C. D. Gilbert, and T. N. Wiesel, “Relationships between horizontal interactions and functional architecture in cat striate cortex as revealed by cross-correlation analysis,” *J. Neurosci.*, vol. 6, pp. 1160–1170, 1986.

[38] C. Gilbert, “Circuitry, architecture, and functional dynamics of visual cortex,” *Cereb. Cortex*, vol. 3, pp. 373–386, 1993.

[39] M. Saam and R. Eckhorn, “Lateral spike conduction velocity in visual cortex affects spatial range of synchronization and receptive field size without visual experience: a learning model with spiking neurons,” *Biol. Cybern.*, vol. 83, L1–L9, 2000.

[40] R. Kempter, W. Gerstner, and J. L. van Hemmen, “Hebbian learning and spiking neurons,” *Phys. Rev. E*, vol. 59, pp. 4498–4514, 1999.

[41] R. Eckhorn, H. J. Reiboeck, M. Arndt, and P. Dicke, “Feature linking via synchronization among distributed assemblies: simulations of results from cat visual cortex,” *Neural Comp.*, vol. 2, pp. 293–307, 1990.

[42] K. Fox and N. Daw, “A model of the action of NMDA conductances in the visual cortex,” *Neural Comput.*, vol. 4, pp. 59–83, 1992.

[43] J. L. Johnson, “Waves in pulse-coupled neural networks,” in *Proc. of the World Congress on Neural Networks*, vol. 4, 1993, pp. 299–302.

[44] J. L. Johnson, “Pulse-coupled neural networks,” in *Proc. of the SPIE Critical Review*, vol. 55, 1994, pp. 47–76.

[45] R. Eckhorn, A. Bruns, M. Saam, A. Gail, A. Gabriel, and H. J. Brinksmeyer, "Flexible cortical gamma-band correlations suggest neural principles of visual processing," *Visual Cogn.*, vol. 8, pp. 519–530, 2001.

[46] W. J. Freeman and J. M. Barrie, "Analysis of spatial patterns of phase in neocortical gamma EEGs in rabbit," *J. Neurophysiol.*, vol. 84, pp. 1266–1278, 2000.

[47] P. Girard, J. M. Hupé, and J. Bullier, "Feedforward and feedback connections between areas V1 and V2 of the monkey have similar rapid conduction velocities," *J. Neurophysiol.*, vol. 85, pp. 1328–1331, 2001.

[48] T. Schanze and R. Eckhorn, "Phase correlation among rhythms present at different frequencies: spectral methods, application to microelectrode recordings from visual cortex and functional implications," *Int. J. Psychophysiol.*, vol. 26, pp. 171–189, 1997.

[49] A. von Stein and J. Sarnthein, "Different frequencies for different scales of cortical integration: from local gamma to long range alpha/theta synchronization," *Int. J. Psychophysiol.*, vol. 38, pp. 301–313, 2000.

[50] A. von Stein, C. Chiang, and P. König, "Top-down processing mediated by interareal synchronization," *Proc. Natl. Acad. Sci. U.S.A.*, vol. 97, pp. 14748–14753, 2000.

[51] B. Schack, N. Vath, H. Petsche, H. G. Geissler, and E. Möller," Phase-coupling of theta-gamma EEG rhythms during short-term memory processing," *Int. J. Psychophysiol.*, vol. 44, pp. 143–163, 2002.

[52] R. Azouz and C. M. Gray, "Cellular mechanisms contributing to response variability of cortical neurons in vivo," *J. Neurosci.*, vol. 19, pp. 2209-2223, 1999.

[53] M. Volgushev, J. Pernberg, and U. T. Eysel, "A novel mechanism of response selectivity of neurons in cat visual cortex," *J. Physiol.*, vol. 540, pp. 307–320, 2002.

[54] M. Häusser and A. Roth, "Estimating the time course of the excitatory synaptic conductance in neocortical pyramidal cells using a novel voltage jump method," *J. Neurosci.*, vol. 17, pp. 7606–7625, 1997.

[55] H. Agmon-Snir and I. Segev, "Signal delay and input synchronization in passive dendritic structures," *J. Neurophysiol.*, vol. 70, pp. 2066–2085, 1993.

[56] M. Nelson, “A mechanism for neuronal gain control by descending pathways,” *Neural Comput.*, vol. 6, pp. 242–254, 1994.

[57] P. König, A. K. Engel, and W. Singer, “Integrator or coincidence detector? The role of the cortical neuron revisited,” *Trends Neurosci.*, vol. 19, pp. 130–137, 1996.

[58] M. Volgushev, M. Chistiakova, and W. Singer, “Modification of discharge patterns of neocortical neurons by induced oscillations of the membrane potential,” *Neurosci.*, vol. 83, pp. 15–25, 1998.

[59] E. D. Lumer, G. M. Edelman, and G. Tononi, “Neural dynamics in a model of the thalamocortical system. II. The role of neural synchrony tested through perturbations of spike timing,” *Cereb. Cortex*, vol. 7, pp. 228–236, 1997.

[60] M. Abeles, *Local Cortical Circuits.* Berlin: Springer, 1982.

[61] A. D. Legatt, J. Arezzo, and H. G. Vaughan, “Averaged multiple unit acticity as an estimate of phasic changes in local neuronal activity: effects of volume-conducted potentials,” *J. Neurosci. Methods*, vol. 2, pp. 203–217, 1980.

[62] C. M. Gray, P. E. Maldonado, M. Wilson, and B. McNaughton, “Tetrodes markedly improve the reliability and yield of multiple single-unit isolation from multi-unit recordings in cat striate cortex,” *J. Neurosci. Methods*, vol. 63, pp. 43–54, 1995.

[63] U. Mitzdorf, “Properties of the evoked potential generators: current source-density analysis of visually evoked potentials in the cat cortex,” *Int. J. Neurosci.*, vol. 33, pp. 33–59, 1987.

[64] R. Eckhorn, “Stimulus-specific synchronizations in the visual cortex: linking of local features into global figures?” in *Neuronal Cooperativity*. Springer Series in Synergetics. J. Krüger, Ed. Berlin: Springer, pp. 184–224, 1991.

[65] W. J. Freeman, L. J. Rogers, M. D. Holmes, and D. L. Silbergeld, “Spatial spectral analysis of human electrocorticograms including the alpha and gamma bands,” *J. Neurosci. Methods*, vol. 95, pp. 111–121, 2000.

[66] E. M. Glaser and D. S. Ruchkin, *Principles of Neurobiological Signal Analysis.* New York: Academic Press, 1976.

FIGURE CAPTIONS

Fig. 1. Coherence of γ-activity is reduced across the representation of an object's contour. **A:** Schema of visual grating stimulus and positions of receptive fields. **B:** A grating without object induced a substantial increase in γ-coherence of local field potentials (LFPs) (light gray) compared to a blank screen condition (pre-stimulus: dashed line). Introduction of the object reduced LFP γ-coherence between inside and outside representations almost to pre-stimulus level from about 100 ms after stimulus onset [16] (dark gray). Coherence within each segment (object or background) remained high (data not shown). **C:** The model (Fig. 14) shows equivalent results. **D,E:** Time course of coherence without object (light gray) and across the figure-ground contour (dark) in the experiment and the model. Note that decoupling across the contour emerges 100 ms after stimulus-onset. Data in **B** is taken from the time intervals with maximal decoupling for each monkey. (Modified from [16, 45].)

Fig. 2. Correct perception of the orientation of a dual-inline row of dots among distractors by a monkey caused a short increase in coherence at about 80 Hz and 60 Hz in visual area V2, shortly before the monkey reported his perception ($t = 0$). The time-frequency map indicates the significance of increase in LFP coherence in trials with correct vs. failed detection of the figure. Three figure-ground stimuli are shown above, with dot rows being left-tilted (left), right-tilted (middle) or absent (right). (Modified from [17].)

Fig. 3. Local field potentials (LFP) at low to medium frequencies in monkey primary visual cortex show modulations related to perceptual switching during binocular rivalry. Visual stimulation was either congruent in both eyes or incongruent, the latter leading to rivalry. Signal modulations were calculated as a function of reported stimulus. Bars: percentage of recording sites showing significant modulations correlated with alternating reports either consistently (light) or oppositely (dark) in both conditions. Percentages refer to the numbers of sites modulated in the congruent condition (numbers

above bars). Asymmetries in favor of co-modulations (light > dark) indicate perception-related modulations only at low to medium frequencies, while stimulus-related modulations (cf. Numbers) also occurred at γ-frequencies.

Fig. 4. γ-waves occur with fast and random changes of spatial phase relations in monkey primary visual cortex. **A:** Simultaneously recorded single-trial time courses of local field potentials (LFPs) from a linear array of 7 recording positions during sustained static visual stimulation. **B:** Model-LFPs during presentation of an equivalent stimulus (cf. Section III-B). (Modified from [45].)

Fig. 5. Velocity distribution of traveling waves of γ-activity measured with 4×4 microelectrode arrays in monkey primary visual cortex.

Fig. 6. The spatial range of γ-waves is larger than that of γ-coherence. **A:** Coherence of local field potentials in monkey primary visual cortex is restricted to few millimeters (half-height decline 2.2 mm). **B:** The probability of continuous γ-waves remains high across larger distances (estimated half-height decline: 9.5 mm). **C, D:** The model shows equivalent dependencies (4.1 vs. 12.8 space units). (Modified from [45].)

Fig. 7. Signal coupling based on envelopes of γ-signals covers larger spatial ranges than coherence of γ-signals proper. Curves show the incidence of coupling events in human intracranial brain signals (as a function of inter-electrode distance) during a visual delayed-match-to-sample experiment (data from 8,500 electrode pairs in 6 subjects). Numbers of significant event-related deviations from baseline are given as multiples of chance level (shaded areas at the bottom of each diagram). *N* refers to the approximate number of independently performed Wilcoxon tests contributing to each data point. *Upper row:* results for different frequency ranges (all tasks). *Lower row:* results for different cognitive tasks in the γ-frequency range.

Fig. 8. Basic model of common spike density modulation in a local population of excitatory neurons by a common inhibitory feedback neuron. Note that first-spike *latencies* in each modulation cycle at the outputs (right) are roughly inversely proportional to the input spike densities (profiles at left), whereas the output spike *rates* are proportional to it (details in text).

Fig. 9. One-dimensional sketch of the initial connectivity in the Hebbian learning model with distance-dependent lateral conduction delays. For a single level-1 neuron (dark), the scheme shows lateral modulatory connections (scenario A), and feed-forward connections with either distance-dependent (scenario B) or constant (scenario C) conduction delays. (Modified from [39].)

Fig. 10. Spatio-temporal properties of level-1 output activity in the Hebbian learning model. **A:** Two events of spatially homogeneous, transient spike-rate enhancement (upper panel: total population spike density; lower panel: single spike traces). **B:** As in A, but with additional independent Gaussian white noise at the inputs. Note that the activity is spatially homogeneous in the sense that any two spike trains have the same weakly correlated temporal statistics. (Modified from [39].)

Fig. 11. Spatial coupling profile between a single level-1 neuron (center position) and its neighbors. **A:** Before learning, weights are randomly initialized. **B:** After learning, synaptic strength decays with increasing distance. (Modified from [39].)

Fig. 12. Due to Hebbian learning the size of the synaptic weight profile (coupling kernel) of lateral linking connections at level-1 becomes directly proportional to the lateral conduction velocity. (Modified from [39].)

Fig. 13: The size of level-1 synchronization fields determines the size of receptive fields of level-2 neurons. Synaptic weight profiles of level-1-to-2 feeding connections evolve correspondingly to synaptic weight profiles of level-1 lateral linking connections. (Modified from [39].)

Fig. 14.: Simplified model of primary visual cortex with two retinotopic layers of orthogonal orientation detectors. Each layer consists of an excitatory (simple cells at 0° and 90°) and an inhibitory sublayer forming fast, local feedback loops preferring the γ-frequency range (Fig. 8). The cones between layers indicate direction and width of divergent projections of each single neuron. Modulatory lateral coupling is confined to excitatory neurons of the same orientation preference with coaxially aligned receptive fields. Both orientation maps share an additional sublayer mediating slow, local shunting inhibition. To account for stochastic input from brain regions excluded from the model, all neurons receive independent broad-band noise. **B:** The spike-coding model neuron with dynamic threshold [41] is extended with inputs exerting shunting inhibition on the feeding pathway. Synapses are modeled by leaky RC-filters, lateral coupling input is offset by +1 (Σ) and then coupled to the feeding pathway by multiplication (Π).

Fig. 15. Temporal dispersion of neural activity can explain the occurrence of envelope-to-signal correlation without corresponding γ-coherence between population signals. Field potentials recorded over or within the source population reflect mean membrane potential fluctuations (upper left), whose γ-frequency components in particular determine the temporal pattern of the generated spikes (lower left). During propagation to the target population, spikes in a bundle of axons are subject to temporal dispersion due to different conduction velocities. This destroys the precise temporal structure of the population spike pattern (lower right). Superposition of postsynaptic potentials elicited in the target population therefore yields field potentials in which only slow spike-density modulations of the source population are reflected (upper right).

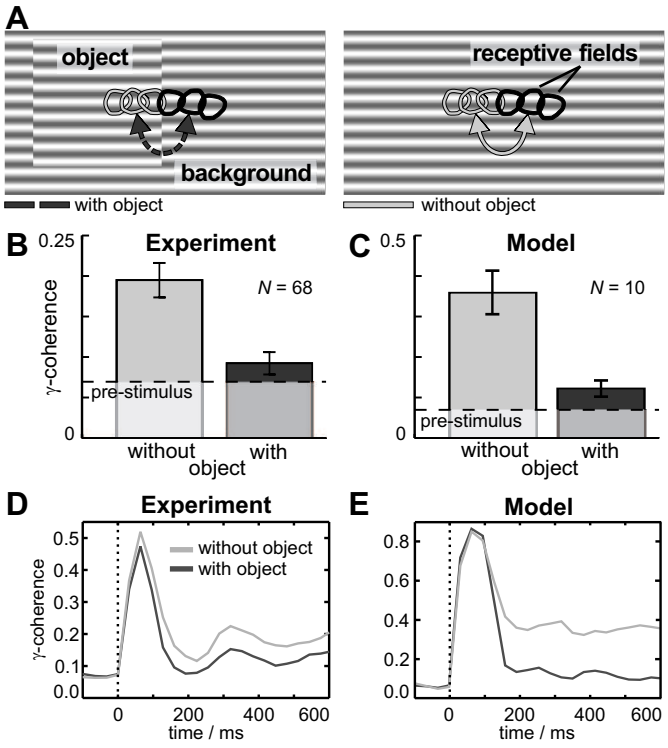

Fig. 1

Eckhorn et al. 2003

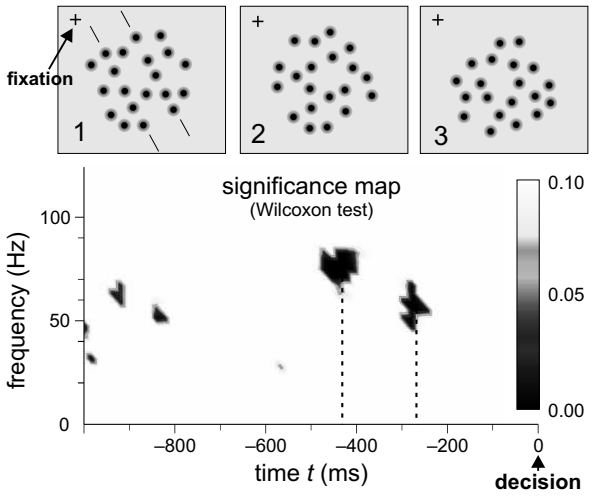

Fig. 2

Eckhorn et al. 2003

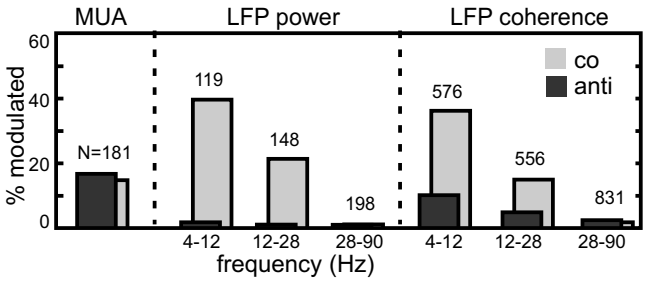

Fig. 3

Eckhorn et al. 2003

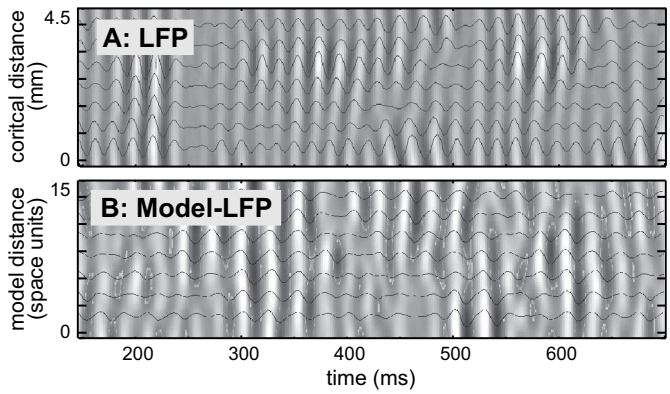

Fig. 4

Eckhorn et al. 2003

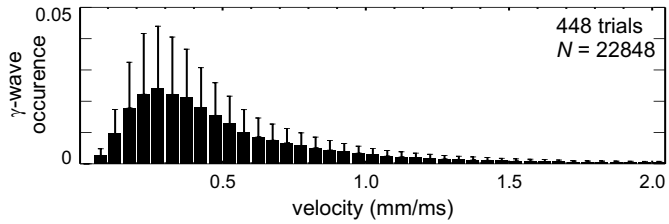

Fig. 5

Eckhorn et al. 2003

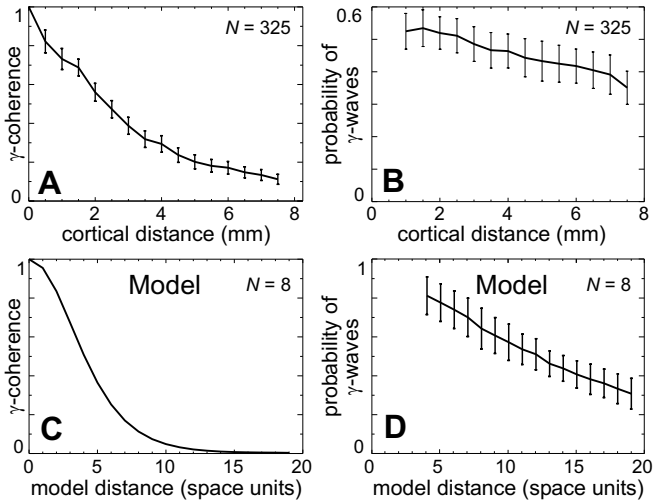

Fig. 6

Eckhorn et al. 2003

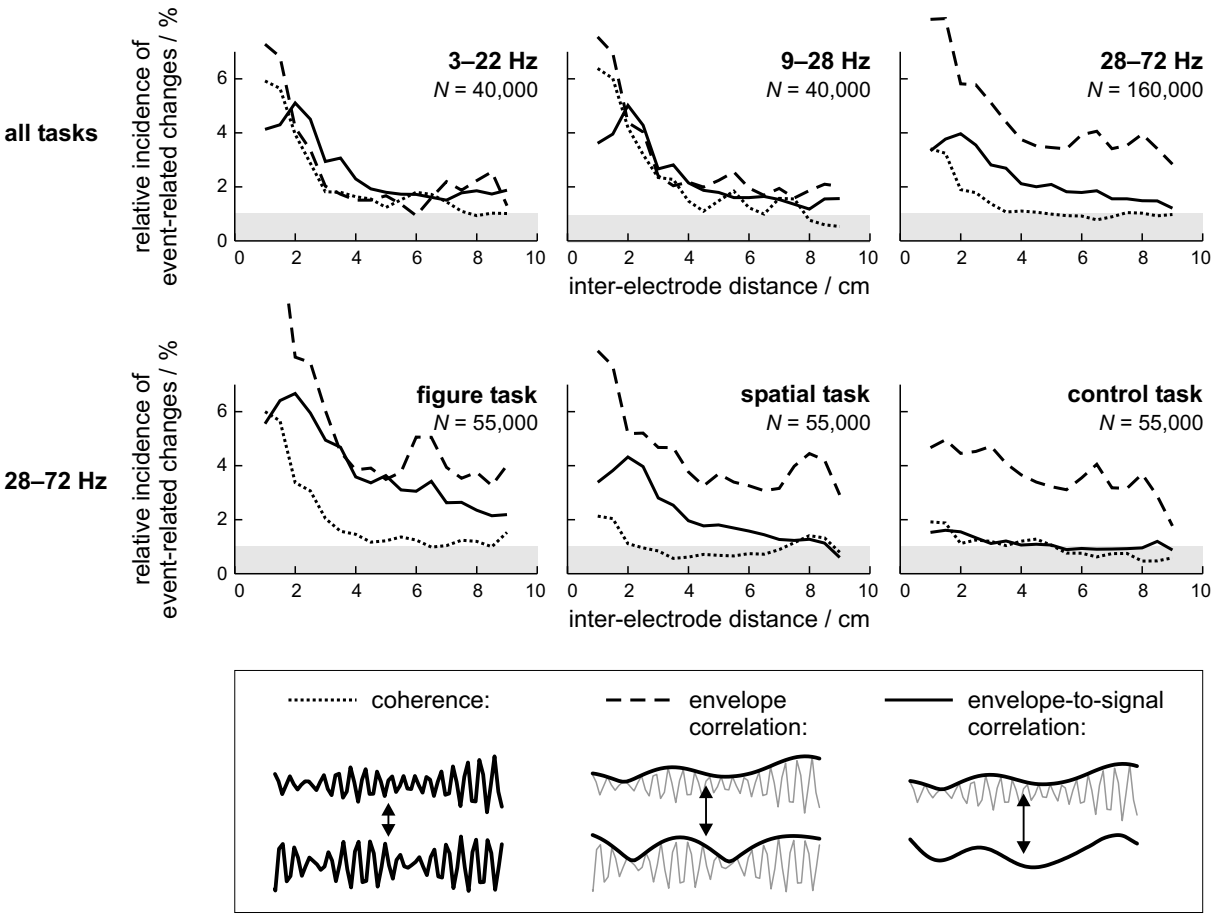

Fig. 7

Eckhorn et al. 2003

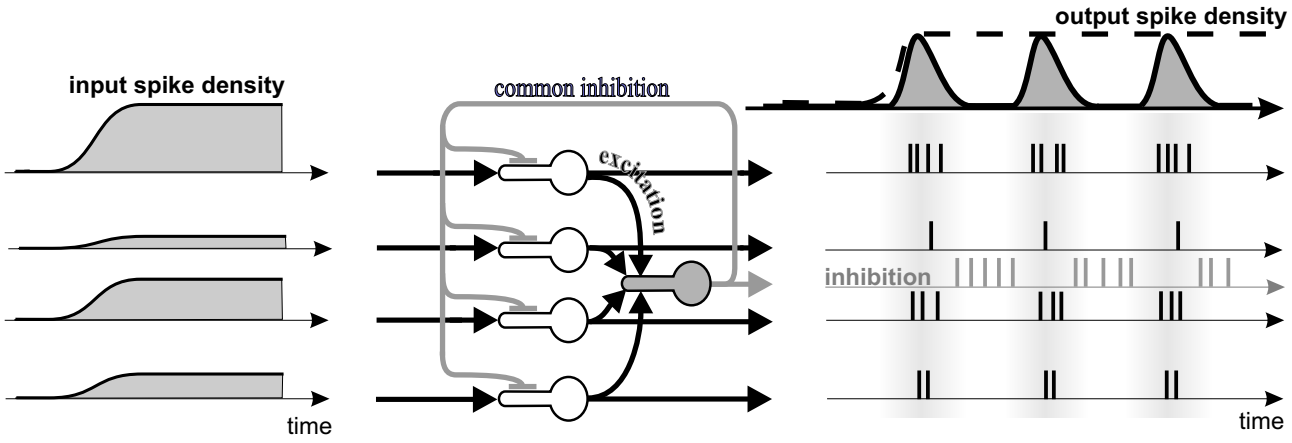

Fig. 8

Eckhorn et al. 2003

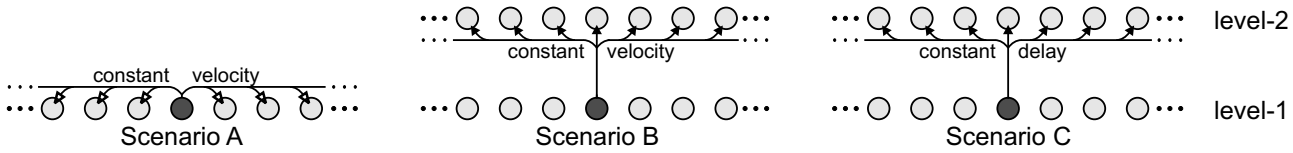

Fig. 9

Eckhorn et al. 2003

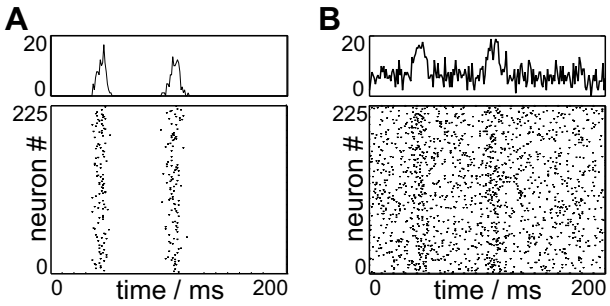

Fig. 10

Eckhorn et al. 2003

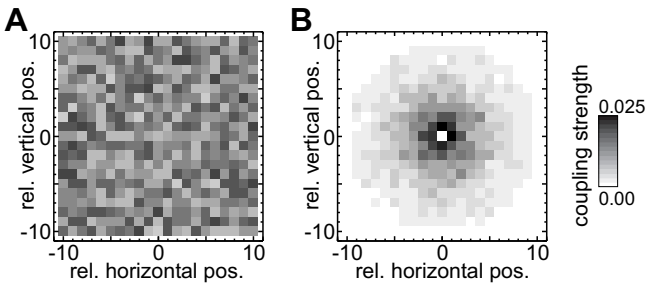

Fig. 11

Eckhorn et al. 2003

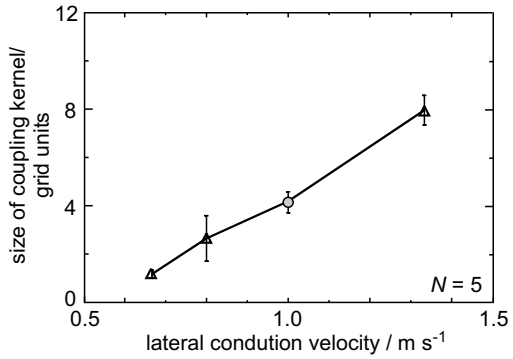

Fig. 12

Eckhorn et al. 2003

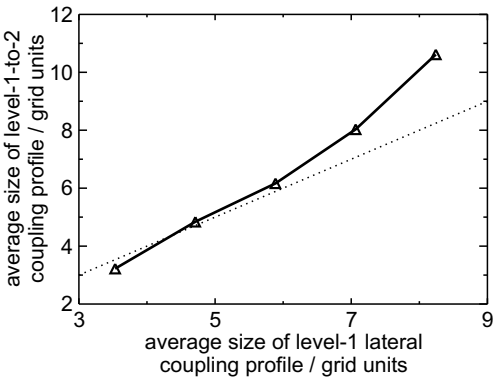

Fig. 13

Eckhorn et al. 2003

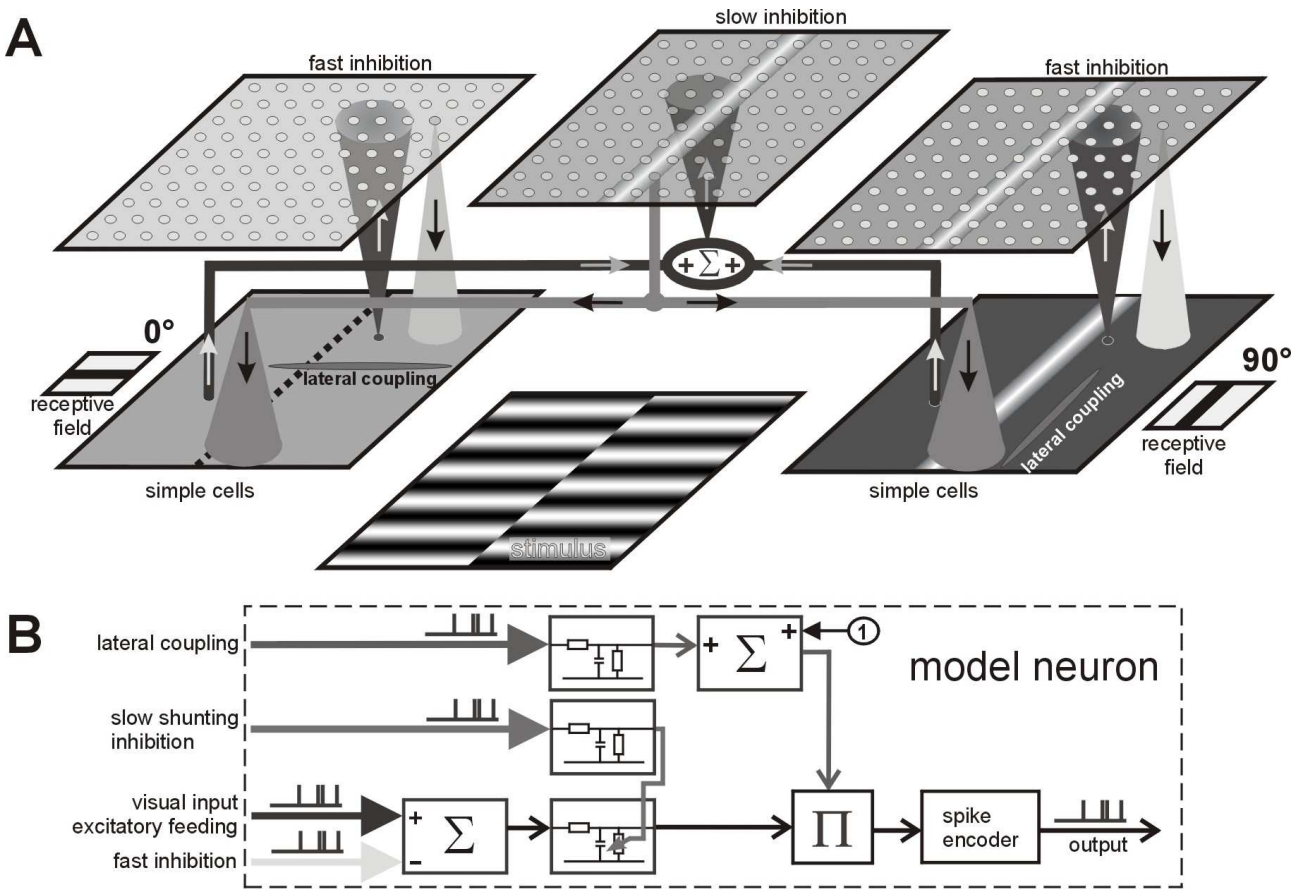

Fig. 14

Eckhorn et al. 2003

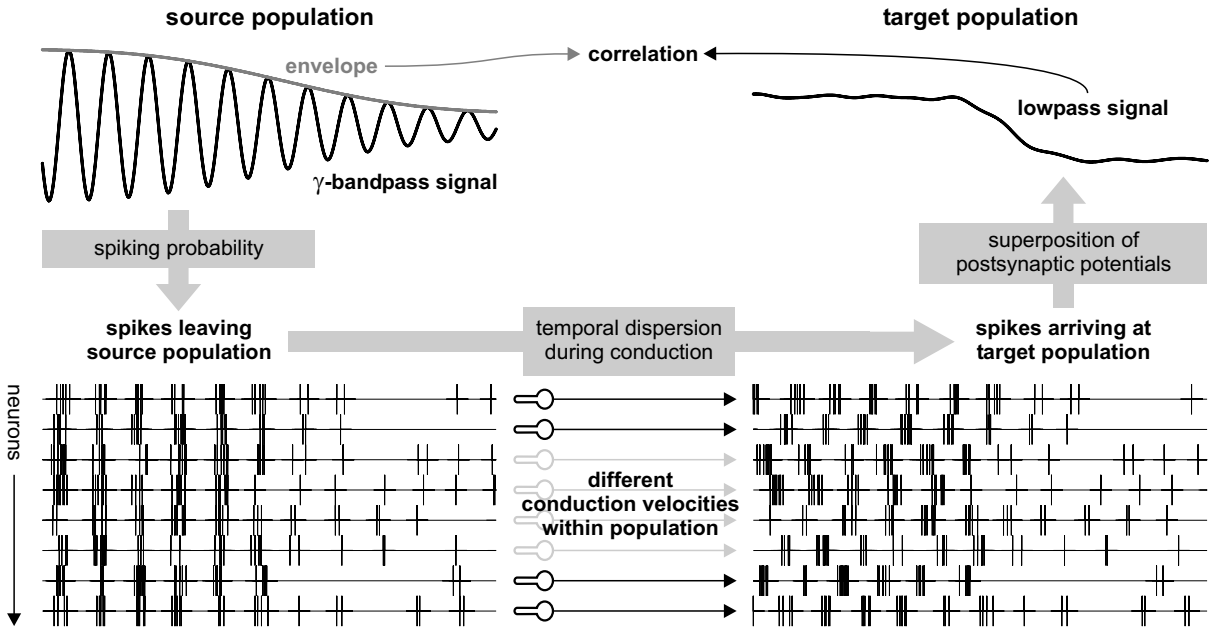

Fig. 15

Eckhorn et al. 2003